Int. Journal of Math. Analysis, Vol. 3, 2009, no. 39, 1923 - 1944

Contact Knots

Ernesto Bribiesca

Departamento de Ciencias de la Computación
Instituto de Investigaciones en Matemáticas Aplicadas y en Sistemas
Universidad Nacional Autónoma de México
Apdo. 20-726, México, D.F., 01000
ernesto@leibniz.iimas.unam.mx

Abstract

We define the contact surface area for tight knots composed of face-connected voxels, which are called contact knots. The contact surface area indicates the area of the surface of the knot which touches itself. A relation between the contact surface area and the area of the surface enclosing the knot is presented. This relation allows us to define a measure of compactness, as initial step, for knot classification. Furthermore, the contact surfaces which are represented by orthogonal 3D (three dimensional) faces generate interesting geometrical patterns for knot analysis.

Mathematics Subject Classification: 57M25

Keywords: contact knots, contact curves, contact surface area, voxelized tight knots, measure of compactness, knot-number notation

1 Introduction

Knot theory is a branch of algebraic topology. The three main techniques of knot theory are: geometric techniques, algebraic tools, and combinatorial methods. A knot K is a simple closed polygonal curve in three-dimensional Euclidean space $\Re^3$ [13]. The study of knots has important applications in the synthesis of new molecules, in DNA research, graph theory, quantum field theory, statistical mechanics, etcetera.

Knots do not necessarily need to be embedded in continuous 3D space. All of them can be implanted into a cubic lattice.

One measure of complexity that is often used is the crossing number, i.e. the number of double points in the simplest planar projection of the knot. Another scale-invariant measure is the quotient of arclength by thickness [4],

i.e. how much "rope" does it take to make a knot [12]. An interesting family of polygonal knots on the cubical lattice is constructed in [7]. A previous measure of compactness for rigid solids was proposed in [3]. Now, here we present a measure of compactness for tight knots composed of face-connected voxels, i.e. voxels with six connectivity. This measure of compactness is based on the relation between the contact surface area (the area of the surface of the knot which touches itself) and the area of the surface enclosing the tight knot.

This paper is organized as follows. In Section 2 we define the contact surfaces. In Section 3 we present the proposed measure of compactness for voxelized tight knots. In Section 4 we define the contact knots. In Section 5 we illustrate some examples of contact knots and their measures of compactness. Finally, in Section 6 we present some conclusions.

2 Contact surfaces

In this section, we present the proposed area relations of tight knots composed of face-connected voxels. The length of all the edges of voxels is considered equal to one. Fig. 1(a) illustrates the left-hand trefoil knot. Fig. 1(b) shows the tight trefoil knot. Fig. 1(c) presents the discrete version of the trefoil knot which is composed of constant orthogonal straight-line segments (in this case, segments were thickened). In order to generate voxelized knots and to obtain contact surfaces, the centroids of voxels are placed with the vertices of the segments of discrete knots. Thus, the voxelized tight trefoil knot is generated, which is shown in Fig. 1(d). The voxelized tight trefoil knot illustrated in Fig. 1(d) is composed of 24 voxels, i.e. $n = 24$.

The voxels have a structural problem, there are three ways of connecting voxels: by edges, vertices, and faces. In the content of this paper we use *face-connected voxels*, i.e. voxels with *six connectivity*. We do not describe the method of digitalization of knots. However, it is important to mention that a rotation-invariant algorithm was used in the digitalization process. This algorithm allows us to align the digitalization grid to the principal axes of the shape of the knot. In this manner, we obtain a description of the shape of the knot invariant under translation and rotation at a given resolution. Using this technique the structural problem of voxels was, in part, eliminated. Thus, for example if a curve is rotated, its description is preserved.

2.1 The total area of the surface of a knot

The total area A_s of the surface of a knot composed of a finite number n of face-connected voxels corresponds to the sum of the areas of the external faces of the voxels of the knot (the external faces correspond to the surface of the

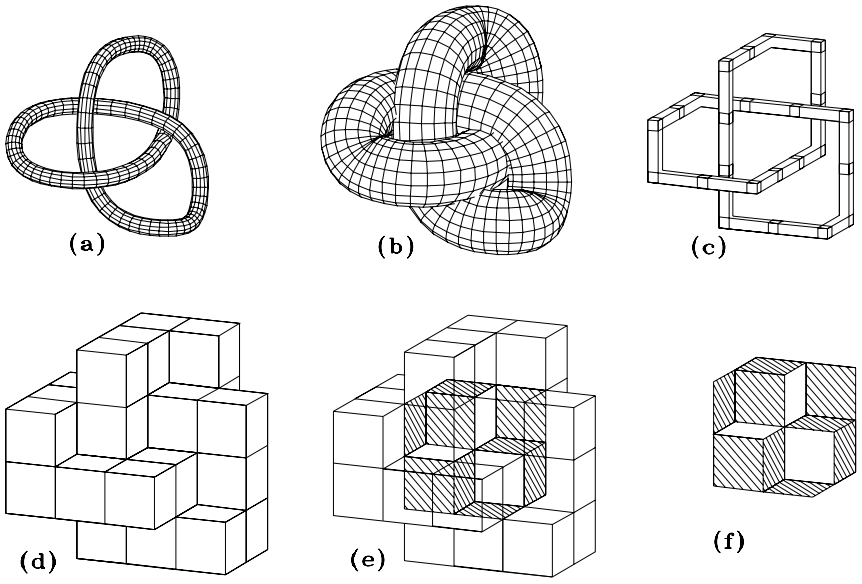

Fig. 1. Contact surfaces: (a) the left-hand trefoil knot; (b) the tight trefoil knot; (c) the discrete version of the trefoil knot; (d) the voxelized trefoil knot; (e)-(f) the contact surfaces of the above-mentioned knot.

knot), i.e. $A_s = 4n$. Thus, the total area of the surface of the knot shown in Fig. 1(d) is equal to 96.

2.2 The area of the enclosing surface

The area A_e of the enclosing surface of a knot composed of a finite number n of face-connected voxels corresponds to the sum of the areas of visible faces of the voxels of the tight knot. We have computed the area of the visible faces of the voxels of the knot shown in Fig. 1(d) and we have obtained that the area of the enclosing surface of the knot is equal to 78 (the number of visible faces of the voxels of the knot).

2.3 The contact surface area

The contact surface area A_c of a knot composed of a finite number n of face-connected voxels corresponds to the sum of the areas of the contact surfaces, i.e. the faces of the voxels of the surface of the knot which touch other voxels. Figures 1(e) and (f) present the contact surfaces which are represented by 3D faces. In this case, the area of the contact surfaces is equal to 9.

2.4 Area relations

Theorem 2.4.1. *For any tight knot composed of n face-connected voxels. The equation*

$$2A_c + A_e = A_s \tag{1}$$

is satisfied.

Geometrically, this means that the sum of twice the contact surface area plus the enclosing surface area is equal to the total sum of the areas of all external faces of the voxels of the tight knot. By Eq.(1), the contact surface area is defined as follows:

$$A_c = \frac{A_s - A_e}{2}. \tag{2}$$

2.5 Contact curves

Definition 2.5.1. *A contact curve is a self-touching curve composed of face-connected voxels, which is constrained to touch itself.*

Each voxel of the curve touches another noncontiguous face-connected or edge-connected voxel of the curve, i.e. the Euclidean distances between the centroids of these voxels always is less than two. Figures 2-5 show examples of contact curves.

2.6 The minimum and maximum contact surface areas

Imagine a snake. In what postures of its body could the snake obtain the minimum and maximum contacts of its skin? In order to find the minimum and maximum contact surface areas for different curves, we have generated different complete families of all closed self-touching curves at different orders (number of voxels) from four to ten, which are presented from Fig. 2 to 5. These complete families of curves are based on previous results obtained in [1]. In a simple closed 3D curve the point of the beginning of the curve is equal to the point of the end. Also, a simple closed curve has no inner crossing [1]. By evaluation all possible orthogonal steps, preserving the contact of voxels, selecting those whose initial and final points are equal, then eliminating those with inner crossings, one obtains the desired family of all closed contact curves. Fig. 2(a) illustrates the family of all closed contact curves of order four. There is only one closed contact curve of order four, which has no contact surfaces. Figures 2(b), (c), and (d) show the family of all closed contact surfaces of order six, in this case there are only three contact curves. In this family of

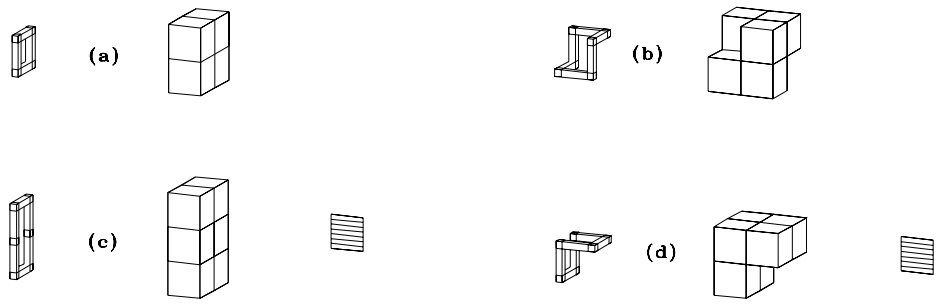

Fig. 2. Family of all closed contact curves of orders four and six, and their contact surfaces: (a) all contact curves of order four; (b)-(d) all contact curves of order six.

curves, the minimum contact surface area corresponds to the contact curve presented in Fig. 2(b). On the other hand, the maximum contact surface area correspond to the curves illustrated in figures 2(c) and (d), which is equal to one.

Fig. 3 shows the family of all closed contact curves of order eight. For instance in these family of order eight, the maximum contact surface area corresponded to the contact curve which describes the first stage of the cube-filling Hilbert curve [8] (in this case, we only use closed cube-filling Hilbert curves), its maximum contact surface area was equal to four (see Fig. 3(m)). On the other hand, in this family of curves there were two curves whose values of contact surface areas were equal to zero (minimum contact surface areas, see figures 3(a) and (b)). In Fig. 3 contact curves were placed in ascending order of contact surface area. Thus, the concept of contact surface area may be a useful tool, as initial step, in curve classification. Figures 4 and 5 show the family of all closed contact curves of order ten. Note that in this family, there are curves which hold the value of the minimum contact surface area equal to zero. On the other hand, there are other contact curves whose maximum contact surface areas are equal to five.

Figure 6 shows an example of a contact curve composed of 64 face-connected voxels. Figures 6(a)-(e) present an example of a curve which has the maximum contact surface area. Fig. 6(a) illustrates the spline curve of the second stage of the cube-filling Hilbert curve. Fig. 6(b) presents the contact curve of the curve shown in (a). Fig. 6(c) shows the second stage of the curve-filling

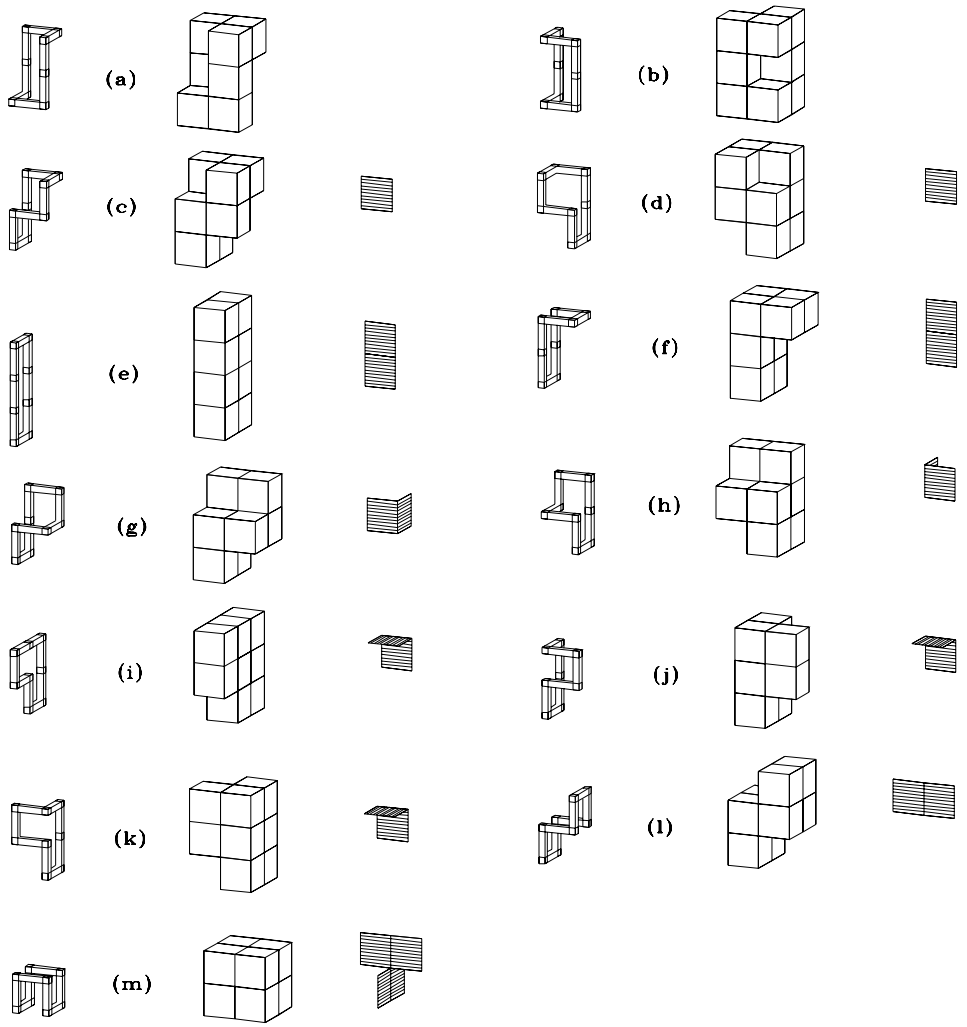

Fig. 3. Family of all closed contact curves of order eight and their contact surfaces: (a)-(m).

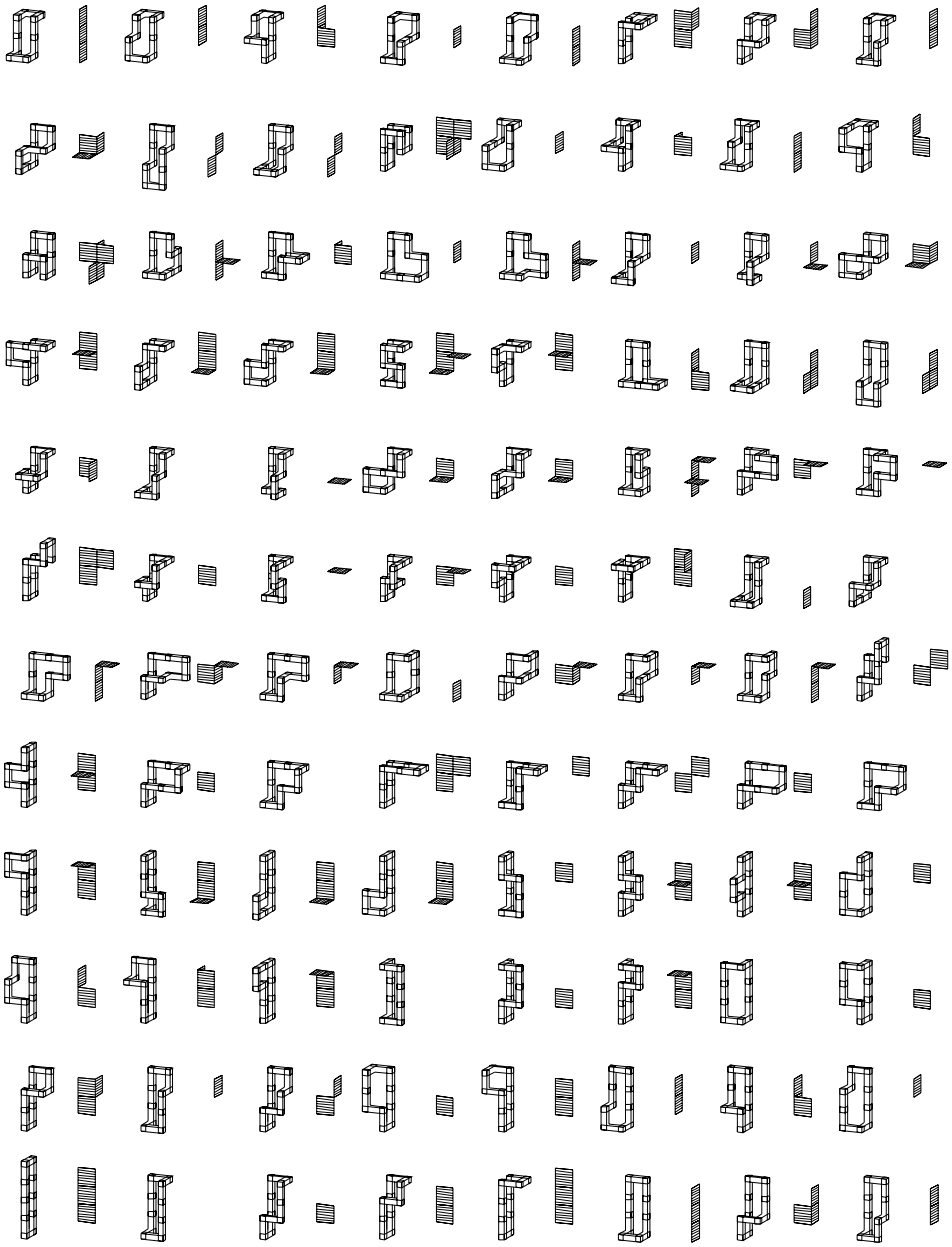

Fig. 4. The first set of the family of all closed contact curves of order ten and their contact surfaces.

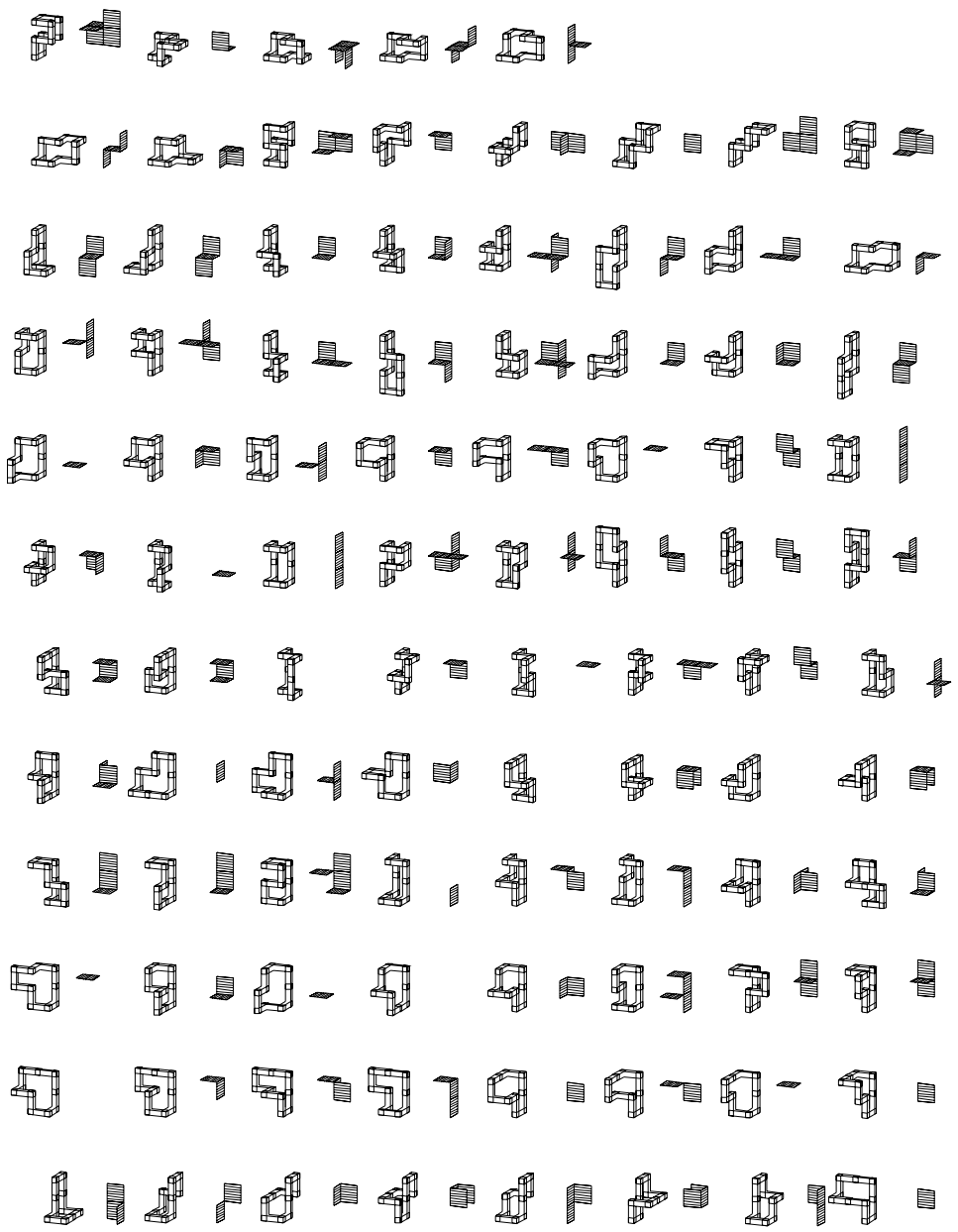

Fig. 5. The second set of the family of all closed contact curves of order ten and their contact surfaces.

Hilbert curve of the family of curves of order 64. A cube-filling Hilbert curve is a classical example of a contact curve. Fig. 6(d) illustrates the voxelized version of the curve shown in (c). Thus, the curve presented in Fig. 6(d) is composed of 64 voxels; its total area is equal to 256; the enclosing surface area is equal to 96; and its contact surface area is equal to 80 (see Fig. 6(e)).

3 The Proposed Measure of Compactness for Voxelized Tight Knots

The compactness of an object is a beautiful property. The compactness for a 2D (two dimensional) shape relates its perimeter p with its area a and can be measured by the ratio $\frac{p^2}{a}$, which is dimensionless and minimized by a disk [9]. In 3D domain, the compactness of an object relates the enclosing surface area a with the volume v and can be defined by the ratio $\frac{a^3}{v^2}$, which is dimensionless and minimized by a sphere. In this work, the term compactness does not refer to point-set topology, but is related to intrinsic properties of objects.

Based on the concept of contact surfaces we define the measure of compactness C for voxelized tight knots as follows:

$$C = \frac{2A_c}{A_s}. \tag{3}$$

The measure of compactness proposed here depends in large part on the sum of the contact surfaces of knots. Thus, this measure indicates a relation between twice the contact surface area and the total area of the surface of the studied knot. The values of this measure of compactness vary continuously from zero to the maximum value of compactness which is always less than one. There is no curve all of whose surface touches itself.

For example, the measure of compactness of the contact curve shown in Fig. 3(a) is equal to zero. This measure of compactness corresponds to the minimum measure of compactness for this family of curves of order 8. On the other hand, the maximum measure of compactness of this family of curves is equal to 0.250000 which corresponds to the curve illustrated in Fig. 3(m), its contact surface area is equal to 4. Table 1 shows the numerical values of the total areas, the areas of the enclosing surfaces, the contact surface areas, and the measures of compactness of the families of all closed contact curves of order four and six shown in Fig. 2. Table 2 presents the numerical values of the total areas, the areas of the enclosing surfaces, the contact surface areas, and the measures of compactness of the family of all closed contact curves of order eight shown in Fig. 3.

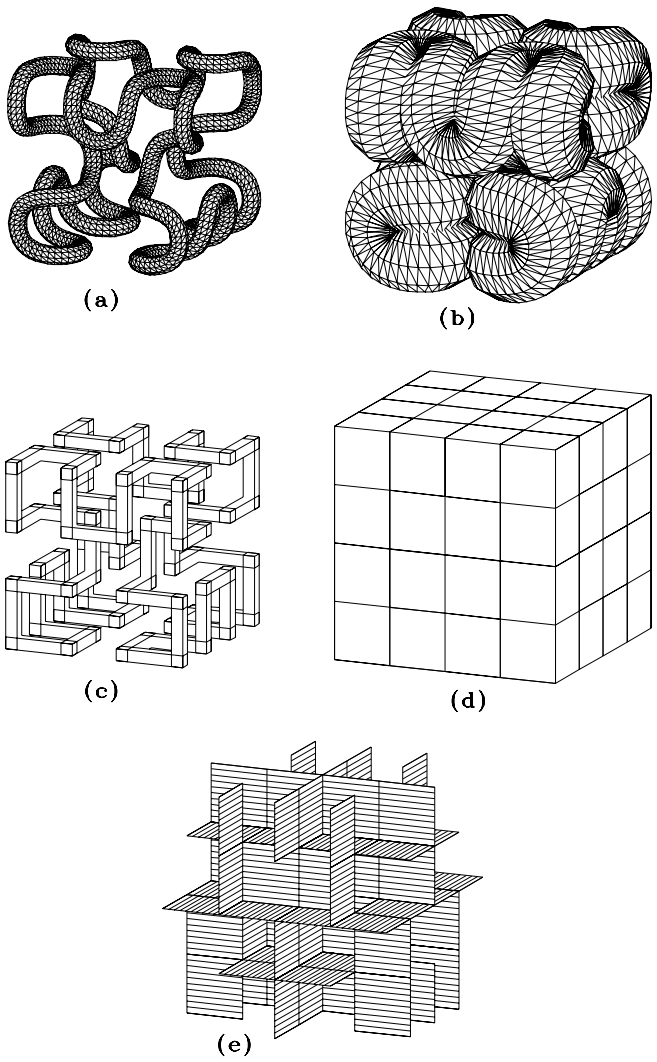

Fig. 6. The maximum contact surface area: (a) the spline curve of the second stage of the cube-filling Hilbert curve; (b) the contact curve of the curve shown in (a); (c) the second stage of the cube-filling Hilbert curve; (d) the above-mentioned curve composed of voxels; (e) the contact surfaces of the cube-filling Hilbert curve.

Curve	n	A_s	A_e	A_c	C
(a)	4	16	16	0	0.000000
(b)	6	24	24	0	0.000000
(c)	6	24	22	1	0.083333
(d)	6	24	22	1	0.083333

Table 1. Numerical values of the areas and measures of compactness of the families of all contact curves of orders four and six.

Curve	n	A_s	A_e	A_c	C
(a)	8	32	32	0	0.000000
(b)	8	32	32	0	0.000000
(c)	8	32	30	1	0.062500
(d)	8	32	30	1	0.062500
(e)	8	32	28	2	0.125000
(f)	8	32	28	2	0.125000
(g)	8	32	28	2	0.125000
(h)	8	32	28	2	0.125000
(i)	8	32	28	2	0.125000
(j)	8	32	28	2	0.125000
(k)	8	32	28	2	0.125000
(l)	8	32	28	2	0.125000
(m)	8	32	24	4	0.250000

Table 2. Numerical values of the areas and measures of compactness of the family of all contact curves of order eight.

4 Contact Knots

A contact knot (voxelized tight knot) is a tight knot composed of face-connected voxels which has no geometric redundancy, i.e. the unit U turn is not accepted (see ref. [2]). For example: figures 7(b), (f), (j), and (n) show contact knots which have no unit U turns. On the other hand, Fig. 6(c) illustrates a contact curve which has several unit U turns. Other example: Fig. 3(e) shows a contact curve which has two unit U turns.

There are many ways for representing contact knots, such as: coordinate systems, 3D arrays of voxels, and chain codes. We have decided to use the *knot-number* notation [1, 2] for representing contact knots. This is due to the fact that knot-number notation has important advantages, such as: it is invariant under *translation* and *rotation*. Also, it is *starting point normalized* and invariant under the *direction of encoding*.

The knot-number notation is based on chain coding. In order to have a self-contained paper, we present the main concepts and definitions of the knot-number notation which is summarized in Appendix A. Initially, this notation was used for describing discrete knots. The main difference between the contact and discrete knots is that the contact knots always touch themselves. Thus, this notation may be used for representing both kinds of knots

A complete review of the above-mentioned notation can be found in [1, 2]. Interesting concepts of knots on the cubic lattice and other representations can be found in [5, 6, 10, 11].

Using the knot-number notation, we generated interesting families of con-

tact curves which allowed us to probe the proposed measure of compactness and obtain interesting geometrical patterns of contact surfaces, as initial step, for knot analysis.

5 Examples of Contact Knots and Their Measures of Compactness

Fig. 7 shows four examples of different contact knots and their measures of compactness. These knots are presented in ascending order of measures of compactness. Fig. 7(a) illustrates the trefoil tight knot. Fig. 7(b) shows the discrete version of the knot shown in (a). In order to facilitate the understanding of contact surfaces, Fig. 7(c) integrates the contact surfaces into the knot shown in (b). Fig. 7(d) illustrates the different values of areas and the measure of compactness of the above-mentioned knot.

Figures 7(e)-(h) show the figure-eight tight knot, its discrete version, its contact surfaces, and its numerical values, respectively. Finally, figures 7(i)-(p) present two more examples of contact knots and their numerical values. The knot with the lowest measure of compactness of the knots presented in Fig. 7 is the trefoil knot illustrated in Fig. 7(a). On the other hand, the knot with the highest measure of compactness of the four knots presented is the knot shown in Fig. 7(m). The smallest nontrivial knot is a trefoil 24 unit long, this knot was proved minimal in 1993 by Diao [5]. This corresponds to the results presented in Fig. 7: the trefoil knot has the lowest measure of compactness of all examples of knots. Notice that the contact surfaces generate different patterns. The contact surface of the trefoil tight knot shown in Fig. 7(c) has three holes. Figures 8(a)-(z) show 26 different configurations of the trefoil contact knot. Figures 9(a)-(z) illustrate the contact surfaces of the contact knots presented in figures 8(a)-(z), respectively. In all 26 different configurations of the trefoil knot, the contact surfaces always preserved three holes in each configuration. The measures of compactness of these configurations of the trefoil tight knot ranged from 0.187500 to 0.291667. Table 3 presents the numerical values of the areas and measures of compactness of the 26 different configurations of the trefoil contact knot shown in Fig. 8. Also, the knot numbers are presented (in this case, we only consider a unique direction of encoding).

The contact surface of the figure-eight tight knot shown in Fig. 7(g) has four holes. Thus, we may use the measure of compactness, the patterns of the contact surfaces, and the number of holes of the contact surfaces, as initial step, for contact-knot classification. Finally, we present a contact curve with a high measure of compactness. Fig. 10 shows the spline curve of the cube-filling Hilbert curve, its contact surface, and both. The discrete version of this curve is composed of 512 face-connected voxels, i.e. $n = 512$, its values of areas are

as follows: $A_s = 2048$, $A_e = 384$, and $A_c = 832$. Therefore, its measure of compactness is equal to 0.812500. Notice that the measure of compactness for the first stage of Hilbert curve is equal to 0.250000, for the second stage is equal to 0.625000, and for the third stage is equal to 0.812500, respectively.

Conjecture 5.1. *When the number of voxels n of contact curves of a family is a perfect cube, Hilbert space filling curves belong to the set of contact curves which hold the maximum contact surface area.*

6 Conclusions

We have introduced a new concept of contact surfaces for voxelized knots. A measure of compactness was defined based on the concept of contact surfaces. This measure of compactness may be a useful tool, as initial step, for curve and knot classification. When the number of voxels n of a family of curves is a perfect cube, we have found that Hilbert curves maximize the numerical values of the measures of compactness.

The contact surfaces generate interesting geometrical patterns for knot classification. For instance, we have detected that the number of holes of any geometrical pattern of a contact knot seems to correspond to the crossing number, i.e. the number of double points in the simplest planar projection of the knot. However, this should be considered as future work.

Appendix A. Knot-Number Notation

In order to have a self-contained paper, we summarize the main concepts and definitions of the knot-number notation.

Definition A.1. *A discrete knot K_D is the digitalized representation of a knot K and is composed of constant orthogonal straight-line segments, whose change directions are described as a chain.*

Definition A.2. *A chain A is an ordered sequence of elements, and is represented by $A = a_1 a_2 \ldots a_n = \{a_i : 1 \leq i \leq n\}$, where n indicates the number of chain elements.*

The chain elements for a discrete knot are obtained by calculating the relative orthogonal direction changes of the contiguous constant straight-line segments along the knot. There are only five possible orthogonal direction changes for representing any discrete knot. Thus, each discrete knot is represented by a chain of elements considered as one base-five integer number, which is called its *knot number*. In this manner, we obtain a unique knot descriptor. Fig. 11(a) illustrates the figure-eight knot. Fig. 11(c) shows the discrete version of

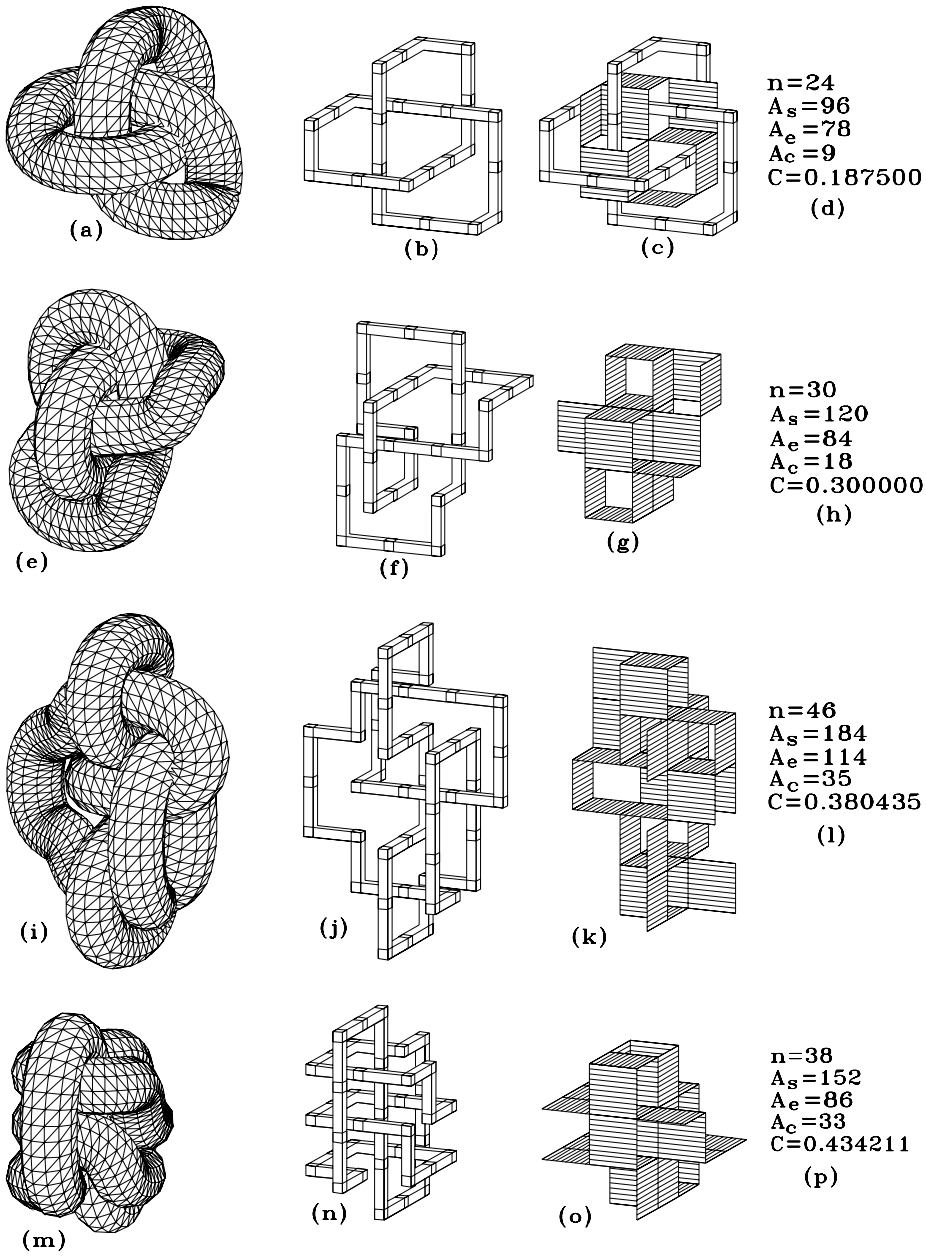

Fig. 7. Four examples of different contact knots: (a)-(d) the trefoil knot, its discrete version, its contact surface, and its values of areas and compactness, respectively; (e)-(h) the figure-eight tight knot and its numerical values of areas and compactness; (i)-(p) another two examples and their areas and measures of compactness.

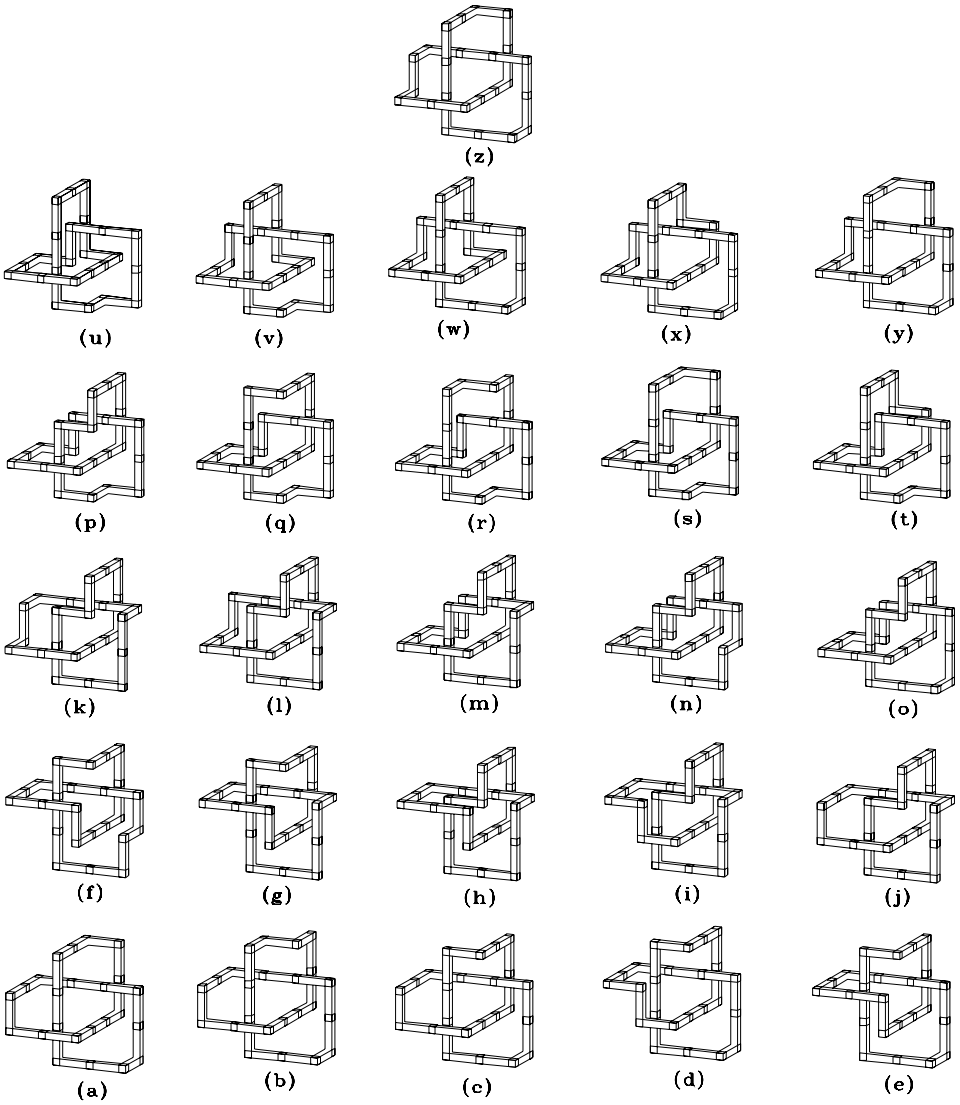

Fig. 8. 26 different configurations of the trefoil contact knot: (a)-(z).

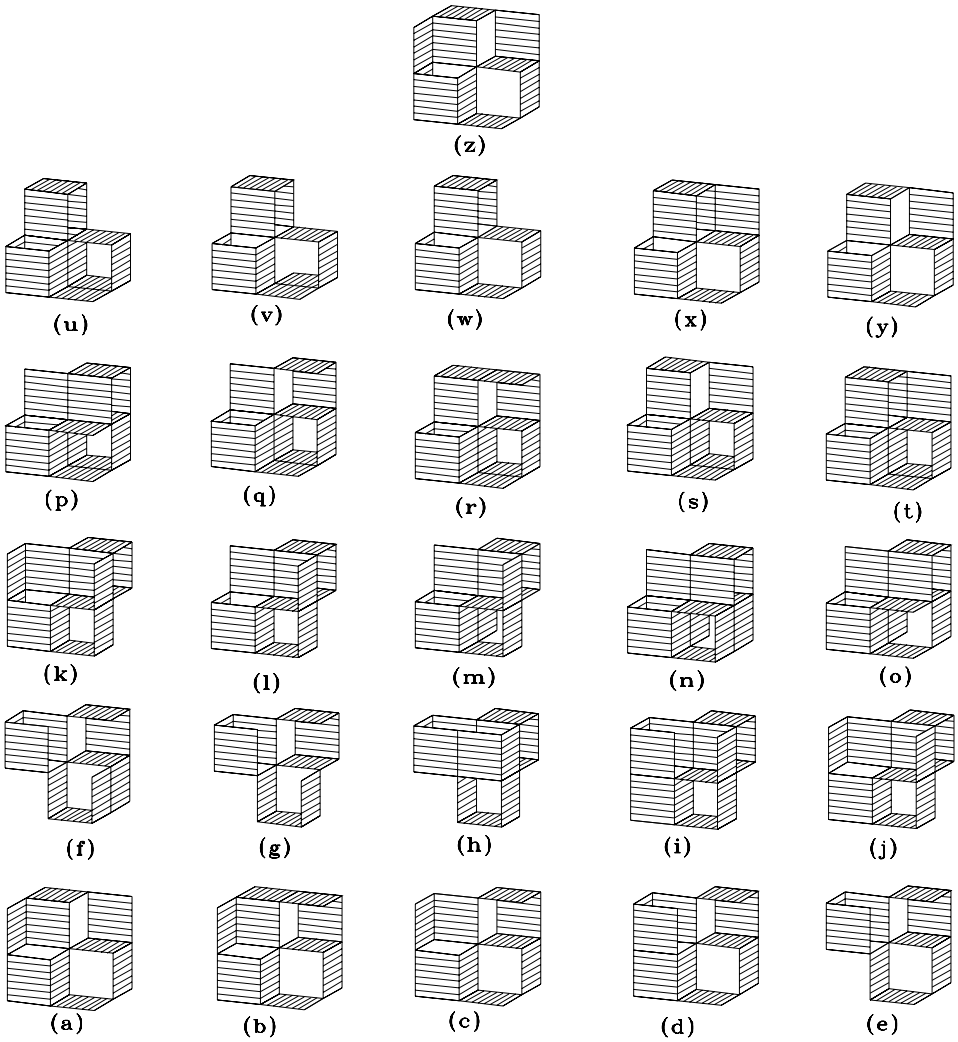

Fig. 9. The corresponding contact surfaces of the different configurations of the trefoil contact knot presented in Fig. 8: (a)-(z), respectively.

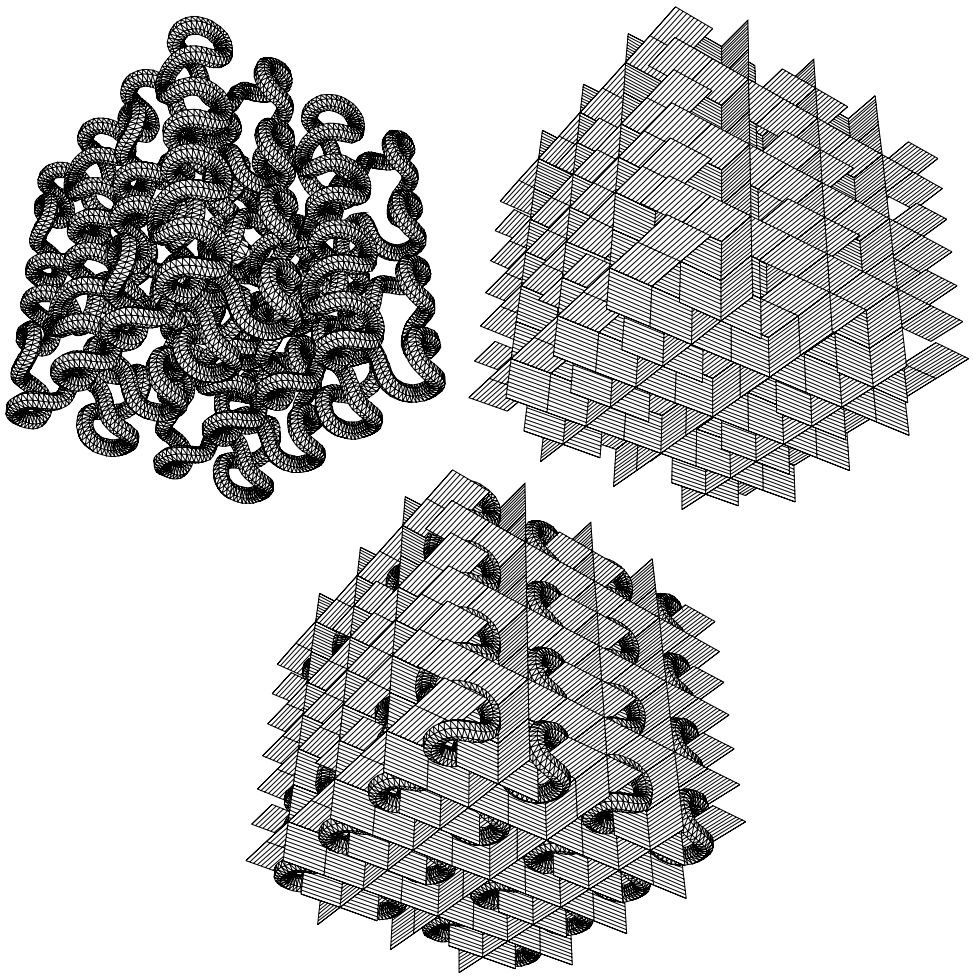

Fig. 10. The spline curve of the third stage of the cube-filling Hilbert curve, its contact surface, and both.

Knot	Knot number	n	A_s	A_e	A_c	C
(a)	00103103001031030010 3103	24	96	78	9	0.187500
(b)	00103103001031030010 4323	24	96	76	10	0.208333
(c)	00103103001040310040 3103	24	96	78	9	0.187500
(d)	00104031004031030010 4323	24	96	76	10	0.208333
(e)	00104031004040310040 3103	24	96	78	9	0.187500
(f)	00104031004040310040 4323	24	96	76	10	0.208333
(g)	00404031004040310040 4031	24	96	78	9	0.187500
(h)	00404031004040432040 4031	24	96	70	13	0.270833
(i)	00104043204040310040 4323	24	96	70	13	0.270833
(j)	00104043204040310040 3103	24	96	72	12	0.250000
(k)	00104043204040310043 2304	24	96	70	13	0.270833
(l)	00104043204040310031 0304	24	96	72	12	0.250000
(m)	00104043204040310323 0404	24	96	68	14	0.291667
(n)	00104043204043230423 0404	24	96	68	14	0.291667
(o)	00104043204031030423 0404	24	96	70	13	0.270833
(p)	00104043204323040423 0404	24	96	68	14	0.291667
(q)	00104031004323040423 0404	24	96	72	12	0.250000
(r)	00104323001323040423 0404	24	96	70	13	0.270833
(s)	00103103001323040423 0404	24	96	72	12	0.250000
(t)	00132304001323040423 0404	24	96	70	13	0.270833
(u)	00104031004040432040 4323	24	96	70	13	0.270833
(v)	00104031004040310040 4323	24	96	76	10	0.208333
(w)	00104031004040310040 3103	24	96	78	9	0.187500
(x)	00104323001040310040 3103	24	96	76	10	0.208333
(y)	00103103001031030041 0304	24	96	78	9	0.187500
(z)	00103103001031030013 2304	24	96	76	10	0.208333

Table 3. The knot numbers, the numerical values, and measures of compactness of the 26 different configurations of the trefoil contact knot shown in Fig. 8.

the knot presented in (a). Thus, this discrete knot is the digitalized version of the figure-eight knot using only constant orthogonal straight-line segments. In the content of this work, we do not describe the method of digitalization. Also, 3D curves are represented as ropes. This improves the understanding of the figures.

An element a_i of a chain, taken from the set $\{0, 1, 2, 3, 4\}$, labels a vertex of the discrete knot and indicates the orthogonal direction change of the polygonal path in such a vertex. Fig. 11(b) summarizes the rules for labeling the vertices: to a straight-angle vertex, a "0" is attached; to a right-angle vertex corresponds one of the other labels, depending on the position of such an angle with respect to the preceding right angle in the polygonal path. Formally, if the consecutive sides of the reference angle have respective directions b and c (see Fig. 11(b)), and the side from the vertex to be labeled has direction d (from here on, by direction, we understand a vector of length 1), then the label or chain element is given by the following function,

$$chain\ element(b, c, d) = \begin{cases} 0, & \text{if } d = c; \\ 1, & \text{if } d = b \times c; \\ 2, & \text{if } d = b; \\ 3, & \text{if } d = -(b \times c); \\ 4, & \text{if } d = -b; \end{cases} \tag{4}$$

where $\times$ denotes the vector product in $\Re^3$.

Thus, the procedure to find the knot number of a discrete knot is as follows:

(i) *Select* an arbitrary vertex of the discrete knot as the origin. Also, *select* a direction for traveling around the discrete knot. Fig. 11(c) illustrates the selected origin which is represented by a sphere. Also, the selected direction is shown and represented by an arrow.

(ii) *Compute* the chain elements of the discrete knot. Fig. 11(c) shows the first element of the chain which corresponds to the element "0". The second element corresponds to the chain element "0", too. The third element corresponds to the chain element "2". Note that when we are traveling around a discrete knot, in order to obtain its chain elements and find zero elements, we need to know what nonzero element was the last one in order to define the next element. In this manner orientation is not lost. Finally, Fig. 11(c) illustrates all chain elements of the figure-eight knot and its chain. It is necessary to have a unique origin for each knot, i.e. this notation is starting point normalized and invariant under the inverse of its chain. The *inverse of a chain* is another chain formed of the elements of the first chain arranged in reverse order (for details see [1]). In order to make this notation invariant under starting point and the inverse of its chain, go to next steps.

(iii) *Choose* the starting point so that the resulting sequence of chain elements forms an integer of minimum magnitude by rotating the digits until the number is minimum. In this case, the selected origin corresponded to the chain elements which formed the integer of minimum magnitude.

(iv) *Select* the opposite direction and go to steps (ii) and (iii). This is shown in Fig. 11(d).

(v) Finally, *select* the minimum integer of the two integers obtained previously. In this case, the minimum integer corresponds to the chain illustrated in Fig. 11(c). The chain of the minimum integer is presented in Fig. 11(e) and this integer is called the *knot number*. Thus, in this stage we have obtained a unique knot descriptor invariant under translation and rotation. Also, it is starting point normalized and invariant under the direction of encoding.

The main characteristics of this knot-number notation are as follows:

(i) It is invariant under translation and rotation. This is due to the fact that only relative orthogonal direction changes are used. Fig. 11(f) illustrates a rotation on the axis "X", of the discrete knot presented in Fig. 11(c). Note that both chains in figures 11(c) and (f) are equal, showing that they are invariant under rotation.

(ii) In this notation, there are only five possible orthogonal direction changes for representing any discrete knot, this produces a numerical string of finite length over a finite alphabet, allows us the usage of grammatical techniques for discrete-knot analysis.

(iii) Using this notation, it is possible to obtain the *mirror image* of a discrete knot with ease. The chain of the mirror image of a discrete knot is another chain (termed the *reflected chain*) whose elements "1" are replaced by elements "3" and vice versa. Fig. 11(g) shows an example of this transformation. In Fig. 11(g) the reflecting plane is aligned with the standard plane "XZ". Notice that the chain elements "1" and "3" of the reflected chain were changed. This change does not depend on the orthogonal reflecting plane used, it is valid for the three possible orthogonal mirroring planes. We do not prove this, only illustrate it [1].

A complete review of the above-mentioned notation can be found in [1, 2].

ACKNOWLEDGEMENTS. I wish to express my gratitude to Richard G. Wilson for his help in reviewing this work. Thanks are also given to Carlos B. Velarde for the generation of chain elements of the third stage of the cube-filling Hilbert curve.

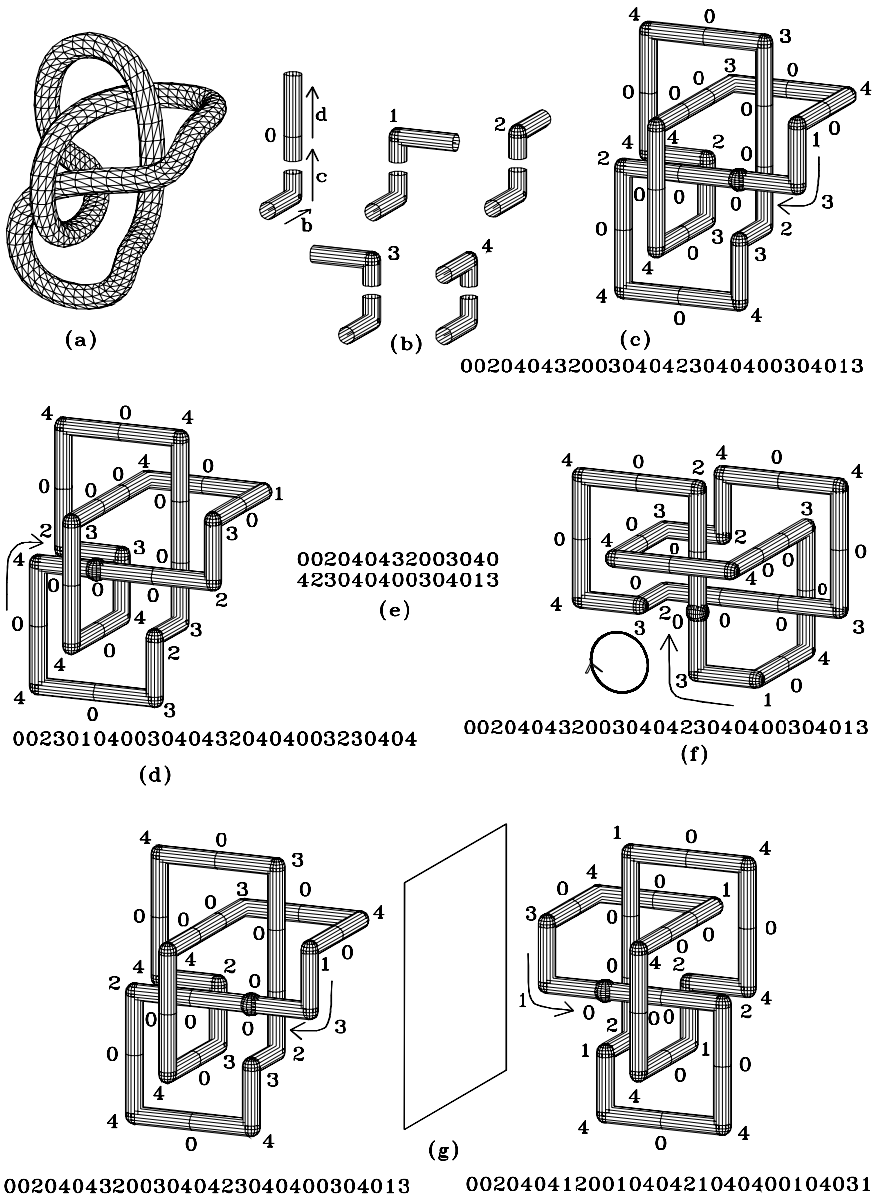

Fig. 11. Knot-number computation: (a) The figure-eight knot; (b) the five possible chain elements; (c) the digitalized version of the knot shown in (a) and its chain; (d) the chain obtained by traveling the discrete knot in the opposite direction; (e) the knot number of the figure-eight knot; (f) independence of rotation, a rotation on the axis "X" of the above-mentioned knot; (g) mirror images of discrete knots, the mirroring plane is aligned with the standard plane "XZ".

References

[1] E. Bribiesca, A Method for computing families of discrete knots using knot numbers, *Journal of Knot Theory and Its Ramifications* **14** (2005), 405-424.

[2] E. Bribiesca, An easy and fast algorithm for obtaining minimal discrete knots, *Journal of Knot Theory and Its Ramifications* **15** (2006), 613-629.

[3] E. Bribiesca, An easy measure of compactness for 2D and 3D shapes, *Pattern Recognition* **41** (2008), 543-545.

[4] J. Cantarella, R. B. Kusner, J. M. Sullivan, Tight knot values deviate from linear relations, *Nature* **392** (1998), 237-238.

[5] Y. Diao, Minimal knotted polygons on the cubic lattice, *Journal of Knot Theory and Its Ramifications* **2** (1993), 413-425.

[6] Y. Diao, The number of smallest knots on the cubic lattice, *Journal of Statistical Physics* **74** (1994), 1247-1254.

[7] Y. Diao, C. Ernst, The complexity of lattice knots, *Topology and its Applications* **90** (1998), 1-9.

[8] W. Gilbert, A cube-filling Hilbert curve, *Mathematical Intelligencer* **6** (1984), 78.

[9] R. C. Gonzalez and R. E. Woods, *Digital Image Processing*, Prentice Hall, Inc., Upper Saddle River, New Jersey 07458, ed. 2, 2002.

[10] B. Hayes, Square knots, *American Scientist* **85** (1997), 506-510.

[11] L. H. Kauffman, Virtual Knot Theory, *Europ. J. Combinatorics* **20** (1999), 663-690.

[12] R. A. Litherland, J. Simon, O. Durumeric, E. Rawdon, Thickness of knots, *Topology and Its Applications* **91** (1999), 233-244.

[13] C. Livingston, *Knot Theory*, The Mathematical Association of America, Washington, DC, 1993.

Received: April, 2009